Available online at www.sciencedirect.com
SCIENCE DIRECT®
Journal of Sound and Vibration 284 (2005) 249–265
JOURNAL OF SOUND AND VIBRATION
www.elsevier.com/locate/jsvi

Structural modification. Part 1: rotational receptances

John E. Mottershead*, Andreas Kyprianou, Huajiang Ouyang

Department of Engineering, Mechanical Engineering Division, The University of Liverpool, Liverpool L69 3GH, UK

Received 25 September 2003; received in revised form 28 April 2004; accepted 15 June 2004

Abstract

The inverse problem of assigning natural frequencies and antiresonances by a modification to the stiffness, mass and damping of a structure is addressed. Very simple modifications such as the addition of masses and grounded springs can be easily accommodated and require the measurement of translational receptances at the connection coordinates. Realistic modifications of practical usefulness, such as a modification by an added beam, require the measurement of rotational as well as translational receptances. Such data are difficult to obtain because of the practical problems of applying a pure moment. One method, the so-called 'T-block' approach, has received considerable attention in the literature, but the accompanying problem of ill-conditioning has not been fully addressed until now. The T-block is attached to the structure at the modification point, so that a force applied to the T-block generates a moment together with a force at the connection point between the T-block and the parent structure. Forces and linear displacements measured on the T-block, together with a mass and stiffness model of the T-block itself, allow the problem to be cast as a special case of excitation by multiple inputs. The resulting equations are generally ill-conditioned, but can be regularized by using a small number of independent measurements. The methodology and signal processing techniques required to estimate the rotational receptances are described. An experimental example is used to demonstrate the practical application of the method.

1. Introduction

Receptances obtained by the processing of data from translational sensors have been readily available for more than two decades and modern modal tests are regularly carried out using

*Corresponding author. Tel.: +44-151-794-4827; fax: +44-151-794-4848.
E-mail address: j.e.mottershead@liv.ac.uk (J.E. Mottershead).

0022-460X/$ - see front matter © 2004 Elsevier Ltd. All rights reserved.
doi:10.1016/j.jsv.2004.06.021

hundreds of data channels. Throughout the 1980s and 1990s the need for rotational receptances intensified for a variety of reasons including the development of procedures for the correlation and updating of finite element models, but most importantly for *structural modification* and *substructure coupling*. A typical case of structural modification is where the dynamic behaviour of a system modified by an added mass or a grounded spring is determined from measurements on the system in its unmodified condition. Simple modifications such as these are entirely described in translational coordinates and require the measurement of translational receptance data only. If a modification is to include a rotational inertia or a rotational stiffness then measured rotational receptances are needed from the unmodified system.

The problem of determining rotational receptances can of course be separated into the two subproblems of (i) measuring rotational motion and (ii) exciting the structure with a moment and measuring it. The first subproblem is the easiest and many papers on rotational measurements concentrate on this aspect. Attempts have been made to apply pure moment excitation, but this is very difficult to achieve in practice. The alternative is to apply a force, which simultaneously imparts a moment, but this is problematic too. Both aspects of rotational receptance estimation are beset with ill-conditioning problems as will be explained in what follows.

Smith [1] used two electromagnetic shakers in a configuration capable of applying a couple by two equal and opposite forces applied to a specially designed fixture. Requirements were described to control the amplification of random experimental errors. Sanderson and Fredo [2] and Sanderson [3] considered bias errors caused by the fixture. These arise from errors in the moment applied to the structure and unwanted excitation of the rotational motion. The former can be corrected by rotational inertia cancellation and the latter depends not only on the design of the moment-excitation fixture but also on the structure itself. Sanderson and Fredo [2] and Sanderson [3] considered fixtures in the form of a T-block and an I-block. Petersson [4] used two giant magnetostrictive alloy rods, excited out of phase with each other to produce a couple on a small T-block, assumed to be a pure moment. Gibbs and Petersson [5] adapted the principle of magnetorestrictive rods to produce a smaller moment actuator to demonstrate the importance of rotational vibrations to structure-born sound. The methodology, together with the necessary equations, required to estimate the moment mobility using the magnetorestrictive actuator are given in detail in Ref. [6]. Su and Gibbs [7] used two-shaker configurations and the magnetostrictive actuator. They concluded that the main drawback of the former stems from the mismatching of forces from the two shakers. A lightweight electromagnetic moment shaker is described in a research report [8] on work carried out under EU contract BRPR-CT97-540. Trethewey and Sommer [9] presented a different way of generating a pure moment by utilizing the couple created by the centrifugal forces of eccentric masses attached to two symmetrically connected rotating wheels. In order to cancel an undesirable moment in an orthogonal direction they added a second identical counter-rotating system of masses on top of the previous one. Bokelberg et al. [10,11] and Stanbridge and Ewins [12] described the measurement of rotational responses by laser sensors and their implementation.

The method described by Ewins and Sainsbury [13], Ewins and Gleeson [14], and Ewins and Silva [15] is amongst the earliest attempts at the measurement of rotational receptances. Using a rigid attachment, such as the T-block, they showed that the full matrix of receptances could be expressed in terms of the measured translational receptances, a coordinate transformation matrix and the mass matrix of the attachment. Cheng and Qu [16] and Qu et al. [17] used a similar

approach, but based upon the use of a rigid 'L'-shaped attachment. Silva et al. [18] proposed a method for the recovery of the rotation-moment receptance from a single column of the receptance matrix corresponding to an applied force. The mass and inertia of the T-block were eliminated by using a substructure coupling technique. Yasuda et al. [19] and Kanda et al. [20] also used a rigid attachment but their studies were concentrated on the measurement of rotational displacements and did not extend to the determination of rotational receptances. Duarte and Ewins [21] considered the transformation matrices for closely spaced accelerometers. Yoshimura and Hosoya [22] determined the rotational receptances by solving an overdetermined least-squares problem using measured time-domain data from a rigid T-block. All methods using rigid fixtures lead to poorly conditioned equations for two reasons: (1) Rotational motion is given by the small difference between translations from accelerometers on the rigid fixture. (2) The excitation points on the rigid fixture are close in comparison to the wavelengths of the modes excited in the structure and therefore the receptances excited from close points on the attachment are very similar. Dong and McConnel [23] relaxed the requirement of a rigid fixture. They determined the full inertance matrix by using a finite element inertance matrix of the T-block together with inertances measured by an instrument cluster (including rotational accelerometers) on the T-block itself.

Ewins [24] showed that the complete matrix of receptances could be determined from measurements of a single row or column, which seems to suggest that the most difficult rotational point receptances are recoverable from other measurements. However Ewins went on to point out the impracticability of his result, since in most cases the measured frequencies are restricted to a range less than the range of natural frequencies of the system and in that case the residuals due to the out-of-range (higher) modes must be included. O'Callahan et al. [25,26] and Avitabile et al. [27,28] used a finite element model to expand the set of measured translational degrees-of-freedom thereby producing an estimate of the unmeasured rotations.

In this paper a multiple-input, multiple-output H_1 estimator is described for rotational receptances using an elastic T-block. The T-block may be quite large since its mass and elasticity properties are included in a finite element model, which allows the displacements and forces (and moments) at the connection point with the main structure to be determined from measurements at accessible points on the T-block where accelerometers and force sensors are located. The resulting estimates are the receptances of the structure under test without any mass, inertia or stiffness effects of the T-block, which are conveniently removed by the T-block finite element model. The use of a large T-block helps with the conditioning of the resulting equations. In addition, the equations may be regularized using independent measurements taken with the T-block removed. The measured data are rich in the natural frequencies of the system with the T-block attached and a further benefit of the regularization is that it tends to counteract this effect. The final result is a multiple-input, multiple-output regularized H_1 estimator, which may be used to determine the full frequency response function matrix at the connection point.

2. Theory

The T-block is connected to the parent structure as shown in Fig. 1 and receptances, including rotational receptances, are required at the connection point 0. The analysis is presented for the

case of vibration in a plane so that the point and transfer receptances at 0 form a 3×3 matrix. The generalization to vibration in three dimensions is a straightforward extension to the theory presented but the equations become more complicated. In that case, a T^2-block is used having perpendicular arms in the form of a cross and the matrix of point and transfer receptances is 6×6. In Fig. 1 the T-block excitation points are shown by arrows and the measured translational responses by black squares.

The equation of motion of the structure may be written so that the dynamic stiffness of the T-block appears on the right-hand side as a forcing term [29],

$$\begin{bmatrix} \mathbf{B}_{11}(\omega) & \mathbf{B}_{10}(\omega) & \\ \mathbf{B}_{01}(\omega) & \mathbf{B}_{00}(\omega) & \\ & & \mathbf{0} \end{bmatrix} \begin{pmatrix} \mathbf{x}_1 \\ \mathbf{x}_0 \\ \mathbf{x}_2 \end{pmatrix} = \begin{pmatrix} \mathbf{0} \\ \mathbf{f}_0 \\ \mathbf{f}_2 \end{pmatrix} - \begin{bmatrix} \mathbf{0} & & \\ & \widetilde{\mathbf{B}}_{00}(\omega) & \widetilde{\mathbf{B}}_{02}(\omega) \\ & \widetilde{\mathbf{B}}_{20}(\omega) & \widetilde{\mathbf{B}}_{22}(\omega) \end{bmatrix} \begin{pmatrix} \mathbf{x}_1 \\ \mathbf{x}_0 \\ \mathbf{x}_2 \end{pmatrix}. \tag{1}$$

The matrix

$$\begin{bmatrix} \mathbf{B}_{11}(\omega) & \mathbf{B}_{10}(\omega) \\ \mathbf{B}_{01}(\omega) & \mathbf{B}_{00}(\omega) \end{bmatrix}$$

is the dynamic stiffness of the parent structure. Subscripts 0 and 1 denote the common coordinates with the T-block at the connection point and the other parent-structure coordinates, respectively. The displacements at the connection point are therefore contained in the vector $\mathbf{x}_0$ and the displacements at the other coordinates are given by the elements of $\mathbf{x}_1$. The matrix

$$\begin{bmatrix} \widetilde{\mathbf{B}}_{00}(\omega) & \widetilde{\mathbf{B}}_{02}(\omega) \\ \widetilde{\mathbf{B}}_{20}(\omega) & \widetilde{\mathbf{B}}_{22}(\omega) \end{bmatrix}$$

is the dynamic stiffness of the T-block. Subscript 2 represents the other T-block coordinates not at the connection point 0. The vectors $\mathbf{f}_0$ and $\mathbf{f}_2$ contain externally applied forces at the connection

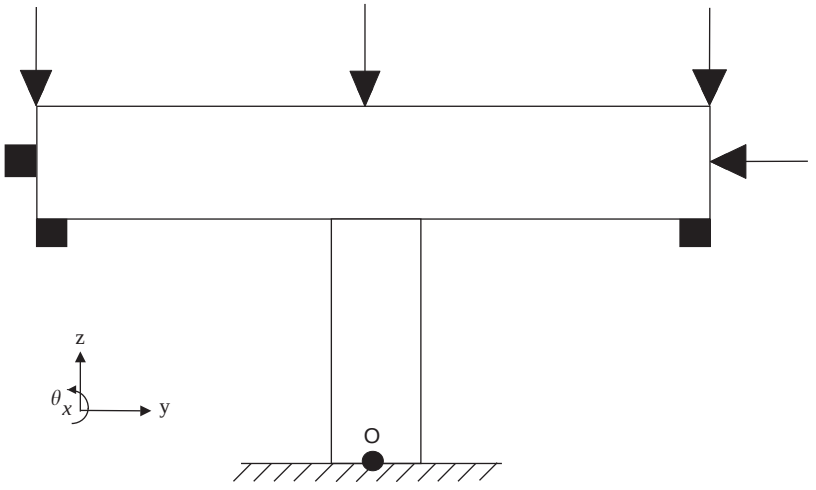

Fig. 1. The T-block attachment.

point and elsewhere on the T-block, respectively. The response vector $\mathbf{x}_0$ may be determined from the last row of Eq. (1),

$$\widetilde{\mathbf{B}}_{20}(\omega)\mathbf{x}_0 + \widetilde{\mathbf{B}}_{22}(\omega)\mathbf{x}_2 = \mathbf{f}_2. \tag{2}$$

Then, assuming $\dim(\mathbf{x}_0) \leqslant \dim(\mathbf{x}_2)$,

$$\mathbf{x}_0 = (\widetilde{\mathbf{B}}_{20}^{*\mathrm{T}}(\omega)\widetilde{\mathbf{B}}_{20}(\omega))^{-1}\widetilde{\mathbf{B}}_{20}^{*\mathrm{T}}(\omega)(\mathbf{f}_2 - \widetilde{\mathbf{B}}_{22}(\omega)\mathbf{x}_2). \tag{3}$$

Now we write the first two rows of Eq. (1) as

$$\begin{bmatrix} \mathbf{B}_{11}(\omega) & \mathbf{B}_{10}(\omega) \\ \mathbf{B}_{01}(\omega) & \mathbf{B}_{00}(\omega) \end{bmatrix} \begin{pmatrix} \mathbf{x}_1 \\ \mathbf{x}_0 \end{pmatrix} = \begin{pmatrix} \mathbf{0} \\ \mathbf{f}_0 - (\widetilde{\mathbf{B}}_{00}(\omega)\mathbf{x}_0 + \widetilde{\mathbf{B}}_{02}(\omega)\mathbf{x}_2) \end{pmatrix}, \tag{4}$$

so that upon premultiplying by the receptance matrix of the parent structure,

$$\begin{pmatrix} \mathbf{x}_1 \\ \mathbf{x}_0 \end{pmatrix} = \begin{bmatrix} \mathbf{H}_{11}(\omega) & \mathbf{H}_{10}(\omega) \\ \mathbf{H}_{01}(\omega) & \mathbf{H}_{00}(\omega) \end{bmatrix} \begin{pmatrix} \mathbf{0} \\ \mathbf{f}_0 - (\widetilde{\mathbf{B}}_{00}(\omega)\mathbf{x}_0 + \widetilde{\mathbf{B}}_{02}(\omega)\mathbf{x}_2) \end{pmatrix} \tag{5}$$

and by extracting the last row of Eq. (5), an equation in the required $\mathbf{H}_{00}$, the matrix of receptances at the connection point, is obtained,

$$\mathbf{x}_0 = \mathbf{H}_{00}(\omega)(\mathbf{f}_0 - (\widetilde{\mathbf{B}}_{00}(\omega)\mathbf{x}_0 + \widetilde{\mathbf{B}}_{02}(\omega)\mathbf{x}_2)). \tag{6}$$

Since $\mathbf{H}_{00}$ is the frequency response function matrix at the connection point 0, it can be deduced that the expression $(\mathbf{f}_0 - (\widetilde{\mathbf{B}}_{00}(\omega)\mathbf{x}_0 + \widetilde{\mathbf{B}}_{02}(\omega)\mathbf{x}_2))$ on the right-hand side of Eq. (6) represents the total system of forces applied to the structure directly and via the T-block. By combining Eqs. (3) and (6) the complete matrix receptance equation for the T-block in terms of measured forces and linear displacement responses may be written as

$$\begin{aligned} &(\widetilde{\mathbf{B}}_{20}^{*\mathrm{T}}(\omega)\widetilde{\mathbf{B}}_{20}(\omega))^{-1}\widetilde{\mathbf{B}}_{20}^{*\mathrm{T}}(\omega)(\mathbf{f}_2 - \widetilde{\mathbf{B}}_{22}(\omega)\mathbf{x}_2) \\ &\quad = \mathbf{H}_{00}(\omega)(\mathbf{f}_0 - (\widetilde{\mathbf{B}}_{00}(\omega)(\widetilde{\mathbf{B}}_{20}^{*\mathrm{T}}(\omega)\widetilde{\mathbf{B}}_{20}(\omega))^{-1}\widetilde{\mathbf{B}}_{20}^{*\mathrm{T}}(\omega) \\ &\qquad \times (\mathbf{f}_2 - \widetilde{\mathbf{B}}_{22}(\omega)\mathbf{x}_2) + \widetilde{\mathbf{B}}_{02}(\omega)\mathbf{x}_2)) \end{aligned} \tag{7}$$

or in simplified form as

$$\mathbf{R}(\omega)\mathbf{f}_2(\omega) + \mathbf{S}(\omega)\mathbf{x}_2(\omega) = \mathbf{H}_{00}(\omega)(\mathbf{f}_0(\omega) + \mathbf{T}(\omega)\mathbf{f}_2(\omega) + \mathbf{U}(\omega)\mathbf{x}_2(\omega)), \tag{8}$$

where

$$\mathbf{R}(\omega) = (\widetilde{\mathbf{B}}_{20}^{*\mathrm{T}}(\omega)\widetilde{\mathbf{B}}_{20}(\omega))^{-1}\widetilde{\mathbf{B}}_{20}^{*\mathrm{T}}(\omega), \tag{9}$$

$$\mathbf{S}(\omega) = -(\widetilde{\mathbf{B}}_{20}^{*\mathrm{T}}(\omega)\widetilde{\mathbf{B}}_{20}(\omega))^{-1}\widetilde{\mathbf{B}}_{20}^{*\mathrm{T}}(\omega)\widetilde{\mathbf{B}}_{22}(\omega), \tag{10}$$

$$\mathbf{T}(\omega) = -(\widetilde{\mathbf{B}}_{00}(\omega)(\widetilde{\mathbf{B}}_{20}^{*\mathrm{T}}(\omega)\widetilde{\mathbf{B}}_{20}(\omega))^{-1}\widetilde{\mathbf{B}}_{20}^{*\mathrm{T}}(\omega)), \tag{11}$$

$$\mathbf{U}(\omega) = \widetilde{\mathbf{B}}_{00}(\omega)(\widetilde{\mathbf{B}}_{20}^{*\mathrm{T}}(\omega)\widetilde{\mathbf{B}}_{20}(\omega))^{-1}\widetilde{\mathbf{B}}_{20}^{*\mathrm{T}}(\omega)\widetilde{\mathbf{B}}_{22}(\omega) - \widetilde{\mathbf{B}}_{02}(\omega). \tag{12}$$

Then, by re-writing Eq. (8) in matrix–vector form for the case of n measurements

$$[\mathbf{R}(\omega) \quad \mathbf{S}(\omega)]\begin{pmatrix}\mathbf{f}_2(\omega)\\ \mathbf{x}_2(\omega)\end{pmatrix}_i = \mathbf{H}_{00}(\omega)[\mathbf{I} \quad \mathbf{T}(\omega) \quad \mathbf{U}(\omega)]\begin{pmatrix}\mathbf{f}_0(\omega)\\ \mathbf{f}_2(\omega)\\ \mathbf{x}_2(\omega)\end{pmatrix}_i, \quad i = 1,2,\ldots,n, \tag{13}$$

and by combining the n equations above

$$[\mathbf{R}(\omega) \quad \mathbf{S}(\omega)]\begin{bmatrix}\mathbf{F}_2(\omega)\\ \mathbf{X}_2(\omega)\end{bmatrix} = \mathbf{H}_{00}(\omega)[\mathbf{I} \quad \mathbf{T}(\omega) \quad \mathbf{U}(\omega)]\begin{bmatrix}\mathbf{F}_0(\omega)\\ \mathbf{F}_2(\omega)\\ \mathbf{X}_2(\omega)\end{bmatrix}, \tag{14}$$

where

$$\mathbf{F}_0(\omega) = [\mathbf{f}_{01}(\omega) \quad \mathbf{f}_{02}(\omega) \quad \ldots \quad \mathbf{f}_{0n}(\omega)], \tag{15}$$

$$\mathbf{F}_2(\omega) = [\mathbf{f}_{21}(\omega) \quad \mathbf{f}_{22}(\omega) \quad \ldots \quad \mathbf{f}_{2n}(\omega)], \tag{16}$$

$$\mathbf{X}_2(\omega) = [\mathbf{x}_{21}(\omega) \quad \mathbf{x}_{22}(\omega) \quad \ldots \quad \mathbf{x}_{2n}(\omega)]. \tag{17}$$

Post-multiplying both sides of Eq. (14) by

$$[\mathbf{F}_0^{*\mathrm{T}}(\omega) \quad \mathbf{F}_2^{*\mathrm{T}}(\omega) \quad \mathbf{X}_2^{*\mathrm{T}}(\omega)]\begin{bmatrix}\mathbf{I}\\ \mathbf{T}^{*\mathrm{T}}(\omega)\\ \mathbf{U}^{*\mathrm{T}}(\omega)\end{bmatrix}$$

leads to

$$\mathbf{B}(\omega) = \mathbf{H}_{00}(\omega)\mathbf{A}(\omega), \tag{18}$$

where

$$\mathbf{A}(\omega) = [\mathbf{I} \quad \mathbf{T}(\omega) \quad \mathbf{U}(\omega)]\begin{bmatrix}\mathbf{G}_{f_0f_0}(\omega)\mathbf{G}_{f_0f_2}(\omega)\mathbf{G}_{f_0x_2}(\omega)\\ \mathbf{G}_{f_2f_0}(\omega)\mathbf{G}_{f_2f_2}(\omega)\mathbf{G}_{f_2x_2}(\omega)\\ \mathbf{G}_{x_2f_0}(\omega)\mathbf{G}_{x_2f_2}(\omega)\mathbf{G}_{x_2x_2}(\omega)\end{bmatrix}\begin{bmatrix}\mathbf{I}\\ \mathbf{T}^{*\mathrm{T}}(\omega)\\ \mathbf{U}^{*\mathrm{T}}(\omega)\end{bmatrix}, \tag{19}$$

$$\mathbf{B}(\omega) = [\mathbf{R}(\omega) \quad \mathbf{S}(\omega)]\begin{bmatrix}\mathbf{G}_{f_2f_0}(\omega)\mathbf{G}_{f_2f_2}(\omega)\mathbf{G}_{f_2x_2}(\omega)\\ \mathbf{G}_{x_2f_0}(\omega)\mathbf{G}_{x_2f_2}(\omega)\mathbf{G}_{x_2x_2}(\omega)\end{bmatrix}\begin{bmatrix}\mathbf{I}\\ \mathbf{T}^{*\mathrm{T}}(\omega)\\ \mathbf{U}^{*\mathrm{T}}(\omega)\end{bmatrix} \tag{20}$$

and the matrices $\mathbf{G}_{f_0f_0}(\omega)$, $\mathbf{G}_{f_0f_2}(\omega),\ldots$ contain spectral densities as indicated by the subscripts.

At this point it should be recalled that there are four separate loading conditions as shown in Fig. 1. Consequently, four equations of the form of Eq. (18) may be written and adding these together a multiple-input, multiple-output MIMO H_1 estimator [30] for the receptances at the T-block point of attachment is expressed as

$$\mathbf{H}_{00}(\omega) = \left(\sum_{k=1}^{4}\mathbf{B}_k(\omega)\right)\left(\sum_{k=1}^{4}\mathbf{A}_k(\omega)\right)^{-1}. \tag{21}$$

The usual requirement for multiple-input, multiple-output frequency response estimation, that the inputs are uncorrelated, may be relaxed in this case. The only requirement being that $\left(\sum_{k=1}^{4}\mathbf{A}_k(\omega)\right)$ is full rank.

3. Finite element model of the T-block

The T-block is a simple structure which we assume can be accurately modelled using finite elements and is represented in Eq. (1) by the dynamic stiffness matrix

$$\begin{bmatrix} \widetilde{\mathbf{B}}_{00}(\omega) & \widetilde{\mathbf{B}}_{02}(\omega) \\ \widetilde{\mathbf{B}}_{20}(\omega) & \widetilde{\mathbf{B}}_{22}(\omega) \end{bmatrix}.$$

Subscripts 0 and 2 represent the coordinates of the connection point and the accelerometer measurement coordinates respectively. The finite element model should include nodes at these coordinates. Finite element nodes at coordinates not included in $\mathbf{x}_0$ and $\mathbf{x}_2$ are unmeasured and therefore need to be eliminated by a model reduction technique.

The finite element model used to produce the results presented in this article consisted of three inextensible Euler–Bernoulli beam elements, and since vibrations only in the plane of the T-block are considered, the particular implementation having two degrees of freedom (one transverse linear and one rotation) at each node is used. Each element has two nodes and hence four degrees of freedom. The assembled T-block model consists of nine degree of freedom as shown in Fig. 2. The unmeasured degrees of freedom θ_7, θ_8 and θ_9 are eliminated using Guyan reduction [31], which causes small rotational inertia effects to be neglected but has the advantage of being independent of frequency.

Care should be taken to ensure the accuracy of the finite element model. The stem of the T-block does not join the top beam at its neutral axis and therefore it is necessary to use an offset

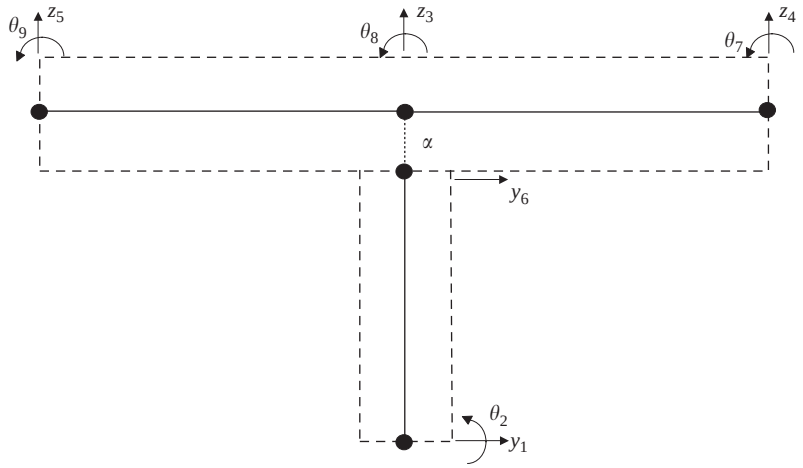

Fig. 2. Complete finite element model of the T-block.

node at the end of the stem. The length of the offset should be half the top-beam depth as indicated by α in Fig. 2. Stiffness and mass matrices for a beam element with such an offset node are given in Ref. [32]. To maintain the mass properties of the element the mass of the top beam should be added to degree-of-freedom y_6 and the mass of the stem to degree of freedom z_3. Accelerometer and force sensor masses should be included. Confirmation of the accuracy of this mass distribution can be obtained from

$$m = \psi_{rb1}^{\mathrm{T}} \mathbf{M} \psi_{rb1}, \tag{22}$$

$$m = \psi_{rb2}^{\mathrm{T}} \mathbf{M} \psi_{rb2}, \tag{23}$$

$$I_G = \psi_{rb3}^{\mathrm{T}} \mathbf{M} \psi_{rb3}, \tag{24}$$

where m and I_G represent the total mass of the T-block (and instrumentation) and its moment of inertia about its centre of gravity. ψ_{rb1}, ψ_{rb2} and ψ_{rb3} are the principal rigid-body modes in directions y, z and pure rotation about the centre of gravity and $\mathbf{M}$ is the mass matrix of the T-block.

4. Experimental arrangement

The experimental rig shown in Fig. 3 takes the form of a portal frame with one leg missing. In the companion paper [33] the sectional properties of the missing leg are determined by an inverse method in order to assign the natural frequencies of the complete system. The initially missing leg is represented by a single Euler–Bernoulli beam element and added to the measured receptances (taken with the leg missing) in order to predict the receptances of the complete portal frame. The predicted receptances are finally confirmed experimentally after the leg has been added to make the portal frame complete. Of course, the Euler–Bernoulli beam has rotational degrees-of-freedom and it is therefore necessary to measure rotational receptances at the connection point with the

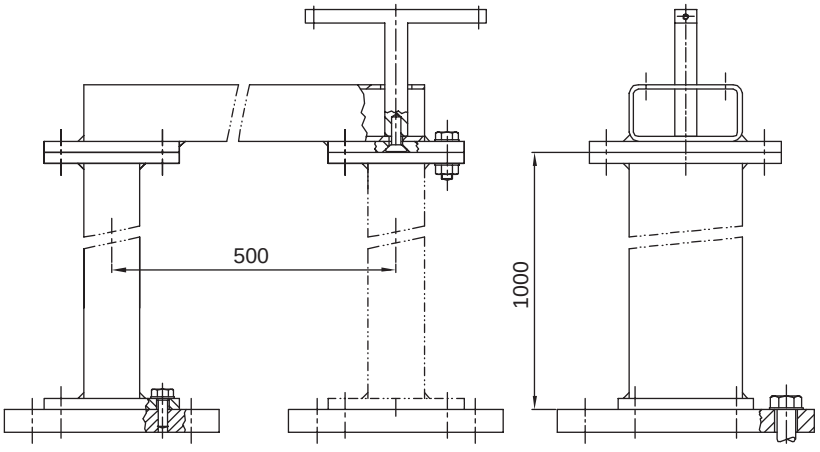

Fig. 3. Experimental set-up.

top beam of the portal frame. The T-block is therefore placed at the free end of the top beam as shown in Fig. 3. The legs and top beam are constructed from 100 mm × 50 mm rectangular hollow steel section with a wall thickness of 4 mm and connections are made by flanges beneath the top beam and at the tops of the legs. The T-bar was connected to the under-top-beam flange using a single M10 set screw. It was anticipated that rotational measurements would be needed with the removable leg in place and for this reason the T-block was fitted from above, requiring a hole to be made in the top beam as shown in Fig. 4. The receptances are therefore estimated at the flange and not at the neutral axis of the top beam.

The T-block has a top beam of length 160 mm, breadth 20 mm and depth 12 mm. The stem is 100 mm long and has a square cross section of 20 mm × 20 mm. Loads were applied to the T-block by an electromagnetic exciter connected in turn to each of the four points shown in Fig. 1. Forces applied to the ends of the T-block arms are entered in the vector $\mathbf{f}_2$ whereas the force at the centre of the top beam is entered into vector $\mathbf{f}_0$ in Eq. (7).

5. Regularization

Most previous researchers assume the T-block to be rigid in the frequency range of interest, which means that it must be very much smaller than the test structure. Then the problem of estimating rotational frequency responses is ill-conditioned for two reasons. Firstly, the rotation is

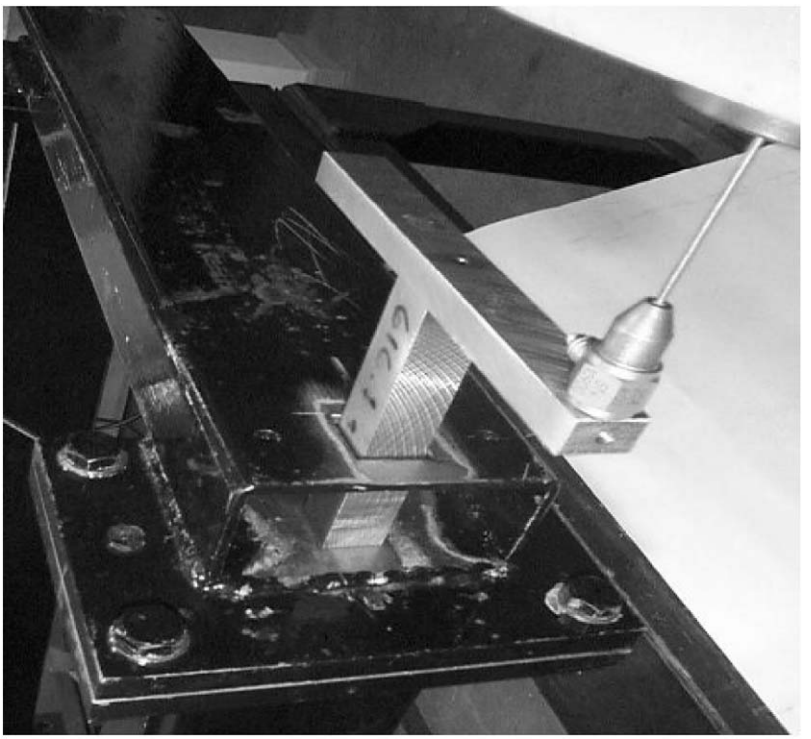

Fig. 4. T-block attachment to the flange.

generally obtained from the small difference of two much larger translational displacements measured at the ends of the T-block arms. Secondly, the receptances at the two arm-ends will be very similar in the range of the lower modes of the test structure. Including the stiffness of the T-block in the formulation allows the use of a larger T-block, which helps with the conditioning. Unfortunately in the particular test described here, one arm-end was unexpectedly found to be close to a vibration node of the second mode in the 'y' direction, which exacerbated the ill-conditioning problem. Tikhonov regularization [34] was applied using the following relationships:

$$\begin{aligned} &h_{yz}(\omega) - h_{zy}(\omega) = 0, \\ &h_{y\theta_x}(\omega) - h_{\theta_x y}(\omega) = 0, \\ &h_{z\theta_x}(\omega) - h_{\theta_x z}(\omega) = 0 \end{aligned} \tag{25}$$

and

$$h_{yy}(\omega) - h^m_{yy}(\omega) = 0. \tag{26}$$

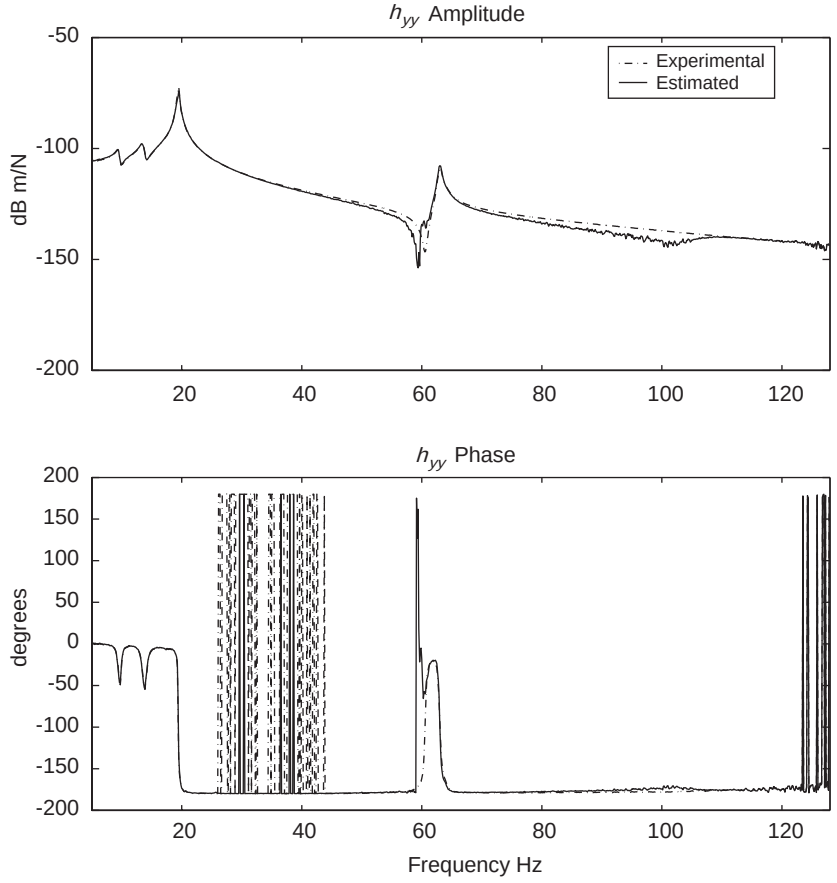

Fig. 5. Measured h^m_{yy} and estimated h_{yy}.

These constraints together with Eq. (14) lead to an objective function of the form

$$\min \left[\sum_{k=1}^{4} \left\| [\mathbf{R}(\omega) \quad \mathbf{S}(\omega)] \begin{bmatrix} \mathbf{F}_2(\omega) \\ \mathbf{X}_2(\omega) \end{bmatrix}_k - \mathbf{H}_{00}(\omega)[\mathbf{I} \quad \mathbf{T}(\omega) \quad \mathbf{U}(\omega)] \begin{bmatrix} \mathbf{F}_0(\omega) \\ \mathbf{F}_2(\omega) \\ \mathbf{X}_2(\omega) \end{bmatrix}_k \right\|_F^2 + \eta((h_{yz}(\omega) - h_{zy}(\omega))^2 + (h_{y\theta_x}(\omega) - h_{\theta_x y}(\omega))^2 + (h_{z\theta_x}(\omega) - h_{\theta_x z}(\omega))^2) + \eta(h_{yy}(\omega) - h_{yy}^m(\omega))^2 \right], \tag{27}$$

where $\| \cdot \|_F$ denotes the Frobenius norm.

A linearity check should be carried out before application of the constraint in Eq. (25). The frequency response $h_{yy}^m(\omega)$ is an independent measurement (without the T-block). Regularization

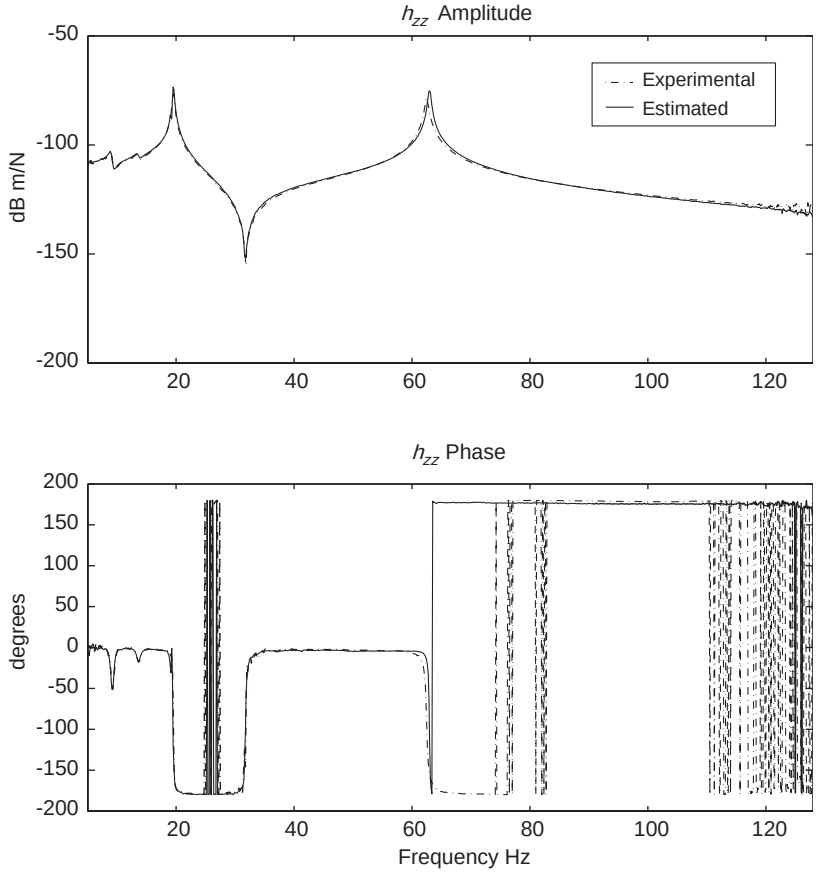

Fig. 6. Measured h_{zz}^m and estimated h_{zz}.

causes constraints to be applied in estimating the required receptances the strengths of which are determined by the magnitude of a regularization parameter η. Of course, different values of η may be applied to the two constraint equations (25) and (26) and other regularizing terms might be added. The measurements are generally very rich in the natural frequencies of the system with the T-block attached and a further advantage of applying a constraint of the form of Eq. (26) is that spurious peaks close to those natural frequencies may be suppressed. Care should be taken in applying regularization since the quality of the estimates and their ability to describe the behaviour of the system may be jeopardized if the value of the regularization parameter is too great.

6. Results

Figs. 5–10 show the estimated receptances obtained by excitation separately at each of the four points shown in Fig. 1. Twenty sequences of time dimain data ($n = 20$) were used at each shaker

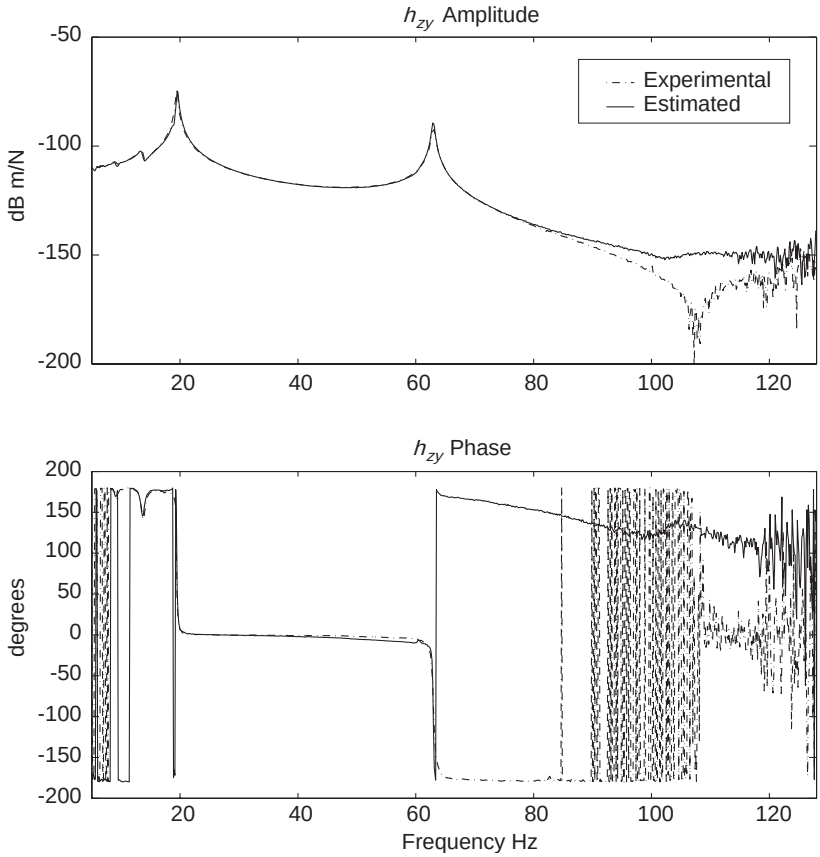

Fig. 7. Measured h_{yz}^{m} and estimated h_{yz}.

location. In Figs. 5–7 a set of receptances measured independently using linear accelerometers at the connection point 0, without the T-block, are overlaid on the estimated receptance curves. It can be seen from Figs. 5 to 7 that the estimated results for the purely translational receptances h_{yy}, h_{zz} and h_{yz}, denoted by the solid line, are in good agreement with the corresponding measured ones, denoted by the dashed line. The cross frequency response functions that include the rotational coordinate were measured using a commercially available rotational accelerometer. These results are compared with the corresponding estimated ones in Figs. 8 and 9. It can be seen that at lower amplitudes of response the results obtained using the rotational accelerometer are noisy and of lower quality than the estimated ones. Fig. 10 shows the sought after rotational frequency response function $h_{\theta_x\theta_x}$ at the connection point 0. This shows a small spurious peak slightly to the left of the second natural frequency of the portal frame. It is possible that the spurious peak can be removed by increasing the weight on the regularization term given by Eq. (26). However if natural frequencies are to be assigned away from the spurious peak in a subsequent structural modification then the presence of the peak in the data is of no importance.

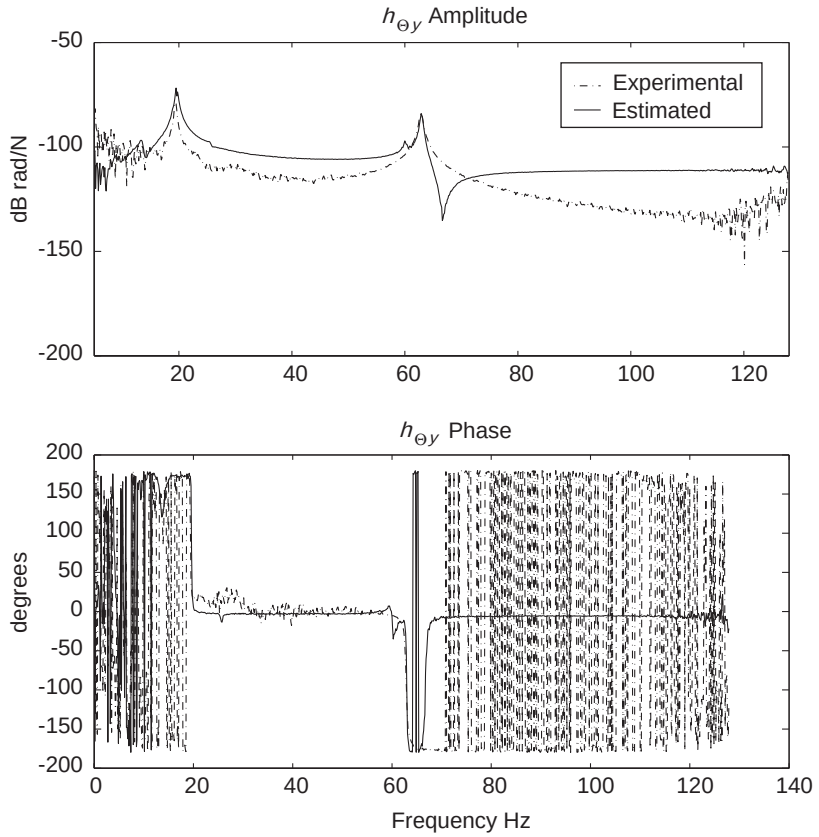

Fig. 8. Measured $h^m_{\theta_x y}$ and estimated $h_{\theta_x y}$.

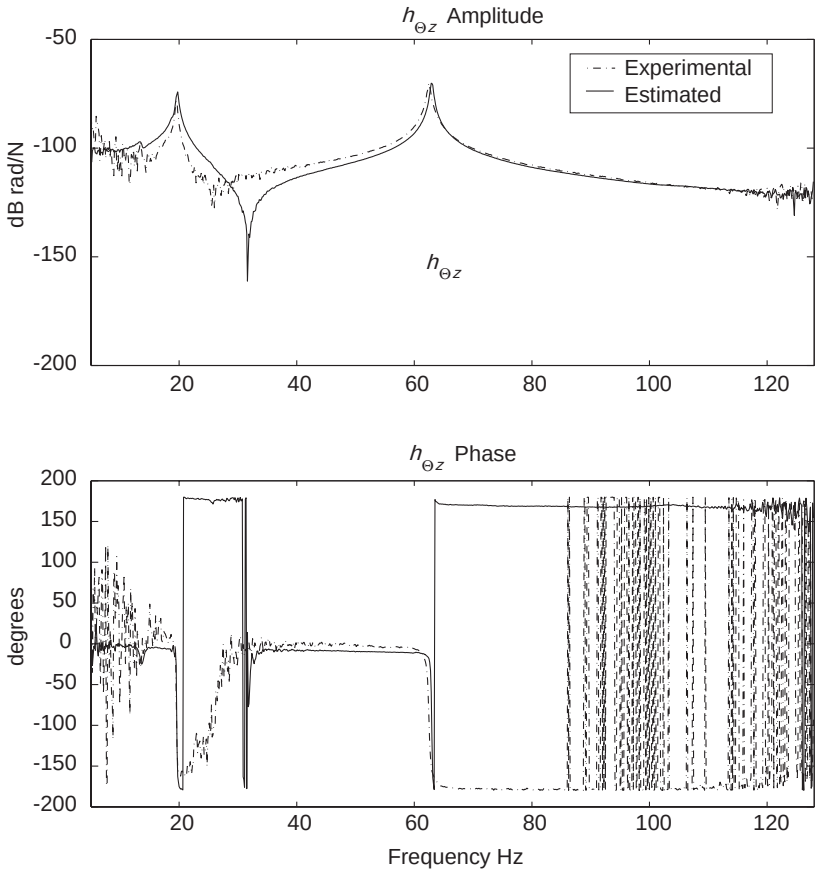

Fig. 9. Measured $h^m_{\theta_x z}$ and estimated $h_{\theta_x z}$.

7. Conclusions

The full 3×3 matrix of receptances for in-plane motion of a beam structure has been determined by a method that uses an elastic T-block. The method requires linear displacement and force measurements at a number of points on the T-block together with a finite element model of the T-block itself. In theory there is no restriction on the size of the T-block and this assists with conditioning of the resulting equations. However the data are rich in the natural frequencies of the system including the T-block, which can itself lead to erroneous results. Generally, it is found to be beneficial to apply regularization using data obtained independently from the structure without the T-block. The primary purpose of the regularization is to alleviate the ill-conditioning but it also has the bonus of removing any bias effects close to the natural frequencies of the system with the T-block present. The resulting over-determined least-squares problem leads to solutions which are applied to the problem of structural modification by an added beam in the companion paper [33].

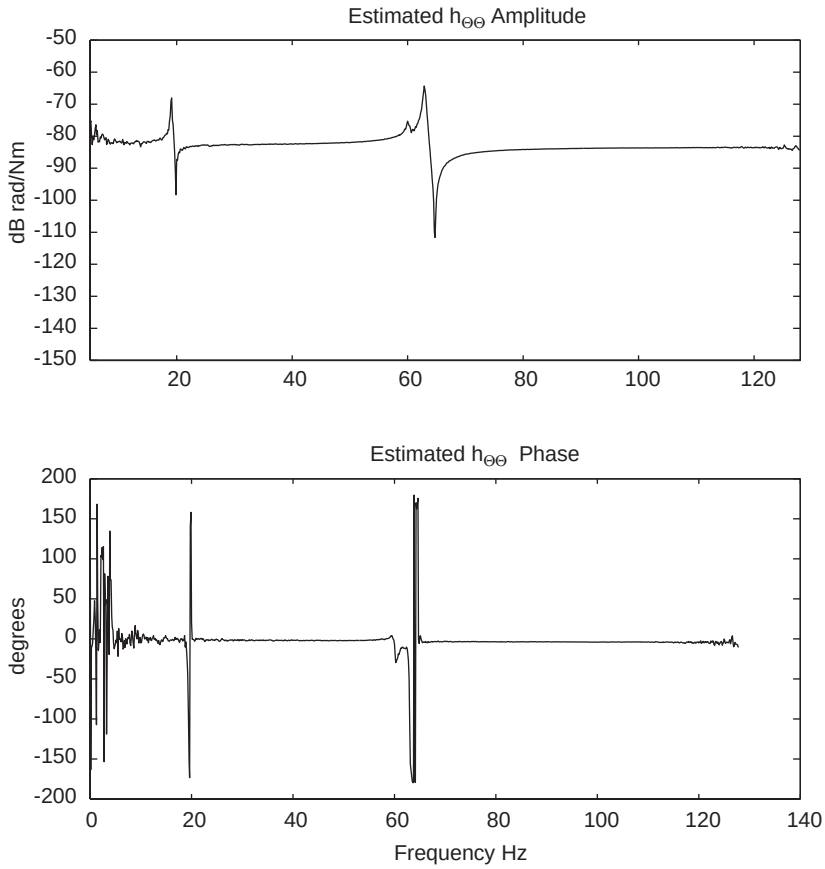

Fig. 10. Estimated rotational receptance $h_{\theta_x\theta_x}$.

References

[1] E.J. Smith, Measurement of the total structural mobility matrix, *Shock and Vibration Bulletin* 40 (7) (1969) 51–84.
[2] M.A. Sanderson, C.R. Fredo, Direct measurement of moment mobility, part I: a theoretical study, *Journal of Sound and Vibration* 179 (4) (1995) 669–684.
[3] M.A. Sanderson, Direct measurement of moment mobility, part II: an experimental study, *Journal of Sound and Vibration* 179 (4) (1995) 685–696.
[4] B. Petersson, On the use of giant magnetostrictive devices for moment excitation, *Journal of Sound and Vibration* 116 (1) (1987) 191–194.
[5] B.M. Gibbs, B. Petersson, Moment excitation and mobility measurement in studies of structure-borne sound emission, *Acoustics Bulletin* 18 (3) (1993) 19–21.
[6] S. Qiu, B.M. Gibbs, B.A.T. Petersson, Measurement of moment mobility using a moment actuator, *Proceedings of Inter-Noise 93*, Leuven, Belgium, August 24–26, pp. 1301–1304.
[7] J. Su, B.M. Gibbs, Measurement of point moment mobility in the presence of non-zero cross mobility, *Applied Acoustics* 54 (1) (1998) 9–26.

[8] EU Contract BRPR-CT97-540, Project Number BE 97-4184, Quantitative treatment and testing of rotational degrees of freedom (QUATTRO): guidelines for experimental techniques, ⟨www.dem.ist.utl.pt/~QUATTRO/⟩.
[9] W.M. Trethewey, H.J. Sommer III, Measurement of rotational DOF frequency response functions with pure moment excitation, *International Conference on Structural Dynamics Modelling*, *Test Analysis*, *Correlation and Validation*, Madeira, Portugal 3–5 June 2002, pp. 81–88.
[10] E.H. Bokelberg, H.J. Sommer III, M.W. Trethewey, A six-degree-of-freedom laser vibrometer, part I: theoretical development, *Journal of Sound and Vibration* 178 (5) (1994) 643–654.
[11] E.H. Bokelberg, H.J. Sommer III, M.W. Trethewey, A six-degree-of-freedom laser vibrometer, part II: experimental validation, *Journal of Sound and Vibration* 178 (5) (1994) 655–667.
[12] A.B. Stanbridge, D.J. Ewins, Modal testing using a scanning laser Doppler vibrometer, *Mechanical Systems and Signal Processing* 13 (2) (1999) 255–270.
[13] D.J. Ewins, M.G. Sainsbury, Mobility measurements for the vibration analysis of connected structures, *The Shock and Vibration Bulletin* 42 (1) (1972) 105–122.
[14] D.J. Ewins, P.T. Gleeson, Experimental determination of multi directional mobility data for beams, *The Shock and Vibration Bulletin* 45 (5) (1975) 153–173.
[15] D.J. Ewins, J.M.M. Silva, Measurements of structural mobility on helicopter structures, Report No. 7909 Dynamics Section, Mechanical Engineering, Imperial College, London, 1979.
[16] L. Cheng, Y.C. Qu, Rotational compliance measurements of a flexible plane structure using an attached beam-like tip, part 1: analysis and numerical simulation, *Journal of Vibration and Acoustics* 119 (1997) 596–602.
[17] Y.C. Qu, L. Cheng, D. Rancourt, Rotational compliance measurements of a flexible plane structure using an attached beam-like tip, part 2: experimental study, *Journal of Vibration and Acoustics* 119 (1997) 603–608.
[18] J.M.M. Silva, N.M.M. Maia, A.M.R. Ribeiro, An indirect method of estimation of frequency response functions involving rotational d.o.f.s, *Proceedings of ISMA 25*, 2000, pp. 1013–1019
[19] C. Yasuda, P.J. Riehle, D.L. Brown, R.J. Allemang, An estimation method for rotational degrees of freedom using a mass additive technique, *Proceedings of IMAC II*, 1984, pp. 877–886
[20] H. Kanda, L.M. Wei, R.J. Allemang, D.L. Brown, Structural dynamic modifications using mass additive technique, *Proceedings of IMAC IV*, 1986, pp. 691–699
[21] M.L.M. Duarte, J.D. Ewins, Rotational degrees of freedom for structural coupling analysis via finite-difference technique with residual compensation, *Mechanical Systems and Signal Processing* 14 (2) (2000) 205–227.
[22] T. Yoshimura, N. Hosoya, FRF estimation on rotational DOFs by rigid block attachment method, *Proceedings of ISMA25*, 2000, pp. 1021–1027
[23] J. Dong, K.G. McConnell, Extracting multi-directional FRF matrices with "Instrument Cluster", *IMAC Proceedings 2002*, pp. 751–764
[24] D.J. Ewins, On predicting point mobility plots from measurement of other mobility parameters, *Journal of Sound and Vibration* 70 (1980) 69–75.
[25] J.C. O'Callahan, I.-W. Lieu, C.-M. Chou, Determination of rotational degrees of freedom for moment transfers in structural modifications, *Proceedings of IMAC III*, 1985, pp. 465–470
[26] J.C. O'Callahan, P. Avitabile, I.-W. Lieu, R. Madden, An efficient method of determining rotational degrees of freedom from analytical and experimental modal data, *Proceedings of IMAC IV*, 1986, pp. 50–58
[27] P. Avitabile, J.C. O'Callahan, C.-M. Chou, V. Kalkunte, Expansion of rotational degrees of freedom for structural dynamic modifications, *Proceedings of IMAC V*, 1987, 950–955
[28] P. Avitabile, J.C. O'Callahan, Frequency response function expansion for unmeasured translation and rotation DOFs for impedance modelling applications, *Mechanical Systems and Signal Processing* 17 (4) (2003) 723–747.
[29] A. Kyprianou, J.E. Mottershead, H. Ouyang, Assignment of natural frequencies by an added mass and one or more springs, *Mechanical Systems and Signal Processing* 18 (2) (2004) 263–289.
[30] J.S. Bendat, A.G. Piersol, *Random Data Analysis and Measurement Procedures*, Wiley, New York, 2000.
[31] R.J. Guyan, Reduction of stiffness and mass matrices, *AIAA Journal* 3 (2) (1965) 380.

[32] J.E. Mottershead, C. Mares, M.I. Friswell, S. James, Selection and updating of parameters for an aluminium space frame model, *Mechanical Systems and Signal Processing* 14 (6) (2000) 923–944.
[33] A. Kyprianou, J.E. Mottershead, H. Ouyang, Structural modification. Part 2: assignment of natural frequencies and antiresonances by an added beam, *Journal of Sound and Vibration* 284 (1 + 2) (2005) 267–281, this issue; doi: 10.1016/j.jsv.2004.06.020.
[34] A.N. Tikhonov, Y.V. Arsenin, *Solutions of Ill-Posed Problems*, Wiley, New York, 1977.